*Int. J. Solids Structures* Vol. 14, pp. 999–1012

0020-7683/78/1201-0999/$02.00/0

# THE LONGITUDINAL HARMONIC EXCITATION OF A CIRCULAR BAR EMBEDDED IN AN ELASTIC HALF-SPACE

G. F. FOWLER
California Institute of Technology, Pasadena, CA 91125, U.S.A.

and

G. B. SINCLAIR
Department of Mechanical Engineering, Carnegie-Mellon University, Pittsburgh, PA 15213, U.S.A.

(*Received* 4 *November* 1977; *in revised form* 5 *April* 1978; *received for publication* 18 *May* 1978)

**Abstract**—This investigation is concerned with the dynamic response of a circular elastic bar of finite length partially embedded in a half-space of distinct elastic properties. The bar is perpendicular to the free surface of the embedding medium and supports a mass which is harmonically excited in the direction of the bar's longitudinal axis. Two bonding conditions are considered: fully bonded wherein the bar completely adheres to the embedding medium throughout the surface of contact, and loosely bonded wherein the bar is secured through its terminal cross section alone. Of primary importance is the energy dissipation due to the spatial characteristics of the embedding medium and accordingly the system is interpreted as a frequency-dependent spring-dashpot.

The determination of the effective spring constant and damping coefficient is achieved by modeling the bar with a one-dimensional theory and using three-dimensional theory for a region which approximates the embedding medium, namely the full half-space. Lamé potentials and Hankel transforms enable a basic half-space problem to be solved which in turn allows integral representations for the spring constant and damping coefficient to be established. For the fully-bonded problem these integral representations involve a bar-force term which must be determined from an integral equation. In both cases the solutions are evaluated numerically over a range of forcing frequencies and for various bar/half-space configurations.

## INTRODUCTION

The problem of interest in this paper is the dynamic response of a right, circular, cylindrical bar of finite length partially embedded in a half-space. The bar's longitudinal axis is perpendicular to the free surface of the half-space. Both the bar and the embedding medium are linear elastic, homogeneous and isotropic, but in general do not have the same elastic constants. The bar is excited in the direction of its *longitudinal axis* by a harmonically oscillating mass at its head. Two bonding conditions on the interface are treated: fully bonded wherein the bar completely adheres to the embedding medium throughout the interface, and loosely bonded wherein the bar is attached through its terminal cross section alone, the remainder of the interface being deemed to be smooth. These two bonding conditions approximate limits for more realistic interface conditions involving friction. Of primary importance is the energy dissipation due to the spatial characteristics of the embedding medium and, given this objective, the problem belongs to a class which seeks to model energy dissipation due to soil-pile interaction during earthquakes. Although the problem is highly idealized, it is thought that the results found will be of some use within this last context and that, moreover, the approach adopted here may prove capable of extension to the more physically relevant problem of the embedded bar under transverse excitation, a problem of some challenge.

Two approaches are available for the analysis of our problem: a finite-element analysis or an analytical approach. Finite-element methods can be adapted to the geometry of the problem in the vicinity of the bar but typically suffer from an inability to adequately handle the infinite medium, especially with respect to energy dissipation. In contrast, analytical approaches usually find the local geometry intractable and must therefore introduce some simplifications; nonetheless, they can accommodate volume energy release due to an infinite embedding medium and it is for this reason we adopt an analytical analysis here.†

†For further comment on the relative merits of the two methods, and an extensive list of references pertaining to dynamic soil-pile interaction, see Hadjian, Luco and Tsai[1].

To date the majority of analytical investigations concerning excitation of embedded bars have rendered the analysis tractable by reducing the dimension of the embedding medium (see for example, Nogami and Novak[2]).† Such dimensional reductions are at variance with our basic aim. *Three-dimensional* analyses of the half-space under *surface* excitation have been furnished by Reissner[3], Bycroft[4] and others (see refs. in [1]). Here is essence we extend Reissner's fundamental solution to the case of the *embedded* bar.

Following the treatment of the static counterpart of our problem by Muki and Sternberg[5], we consider a one-dimensional theory for the bar and three-dimensional theory for a region approximating the embedding medium, namely the entire half-space. In Section 1 we describe our problem, emphasizing its interpretation as an equivalent frequency-dependent spring-dashpot, and derive an integral equation relating forces and displacements for the fully-bonded bar. In Section 2 we establish integral representations for the effective spring constant and equivalent damping coefficient for both bonding conditions (drawing on an analysis of an underlying half-space problem given in the Appendix) and describe the numerical solution of the associated integral equation. Results are presented for a range of forcing frequencies and for various bar/half-space configurations in Section 3. The results indicate the dependence on embedment, on a ratio of the wave speeds for the bar and half-space and on a ratio of densities.

## 1. APPROXIMATE FORMULATION OF THE PROBLEM

In this section we formulate a mathematical model for an embedded bar supporting a mass under periodic loading. The global characteristics of the problem are discussed before we describe the mass, bar and embedding medium in turn for the fully-bonded system. The formulation is then specialized to the loosely-bonded case.

Let $(r, z)$ be an axisymmetric cylindrical coordinate system with $z$-axis perpendicular to the surface of the embedding medium and positive downwards (Fig. 1). The plane of the free surface of the embedding medium intersects the $z$-axis at the origin $O$. The embedding region $\mathscr{R} = \{(r, z) | r > d/2,\ 0 < z \leqslant D \text{ or } r \geqslant 0,\ z > D\}$ is a linear elastic, homogeneous and isotropic half-space with a right, circular, cylindrical cavity of diameter $d$ and depth $D$, the longitudinal axis of which coincides with the $z$-axis. The region $\mathscr{B} = \{(r, z) | 0 \leqslant r < d/2,\ -(L-D) < z < D\} (D \leqslant L)$ is a homogeneous and isotropic circular bar of distinct elastic properties with diameter $d$ and length $L$ which sits in the cavity in $\mathscr{R}$; a cross section of $\mathscr{B}$ is the disk $\mathscr{D}_z = \{(r, z) | 0 \leqslant d/2,\ z \text{ held constant}\}\ (-(L-D) \leqslant z \leqslant D)$. We say the bar $\mathscr{B}$ is *fully bonded to* the embedding region $\mathscr{R}$ if $\mathscr{B}$ adheres to $\mathscr{R}$ perfectly throughout the entire contact surface $\partial\mathscr{R} \cap \partial\mathscr{B}$, $\partial\mathscr{R}$ and $\partial\mathscr{B}$ being the surfaces of $\mathscr{R}$ and $\mathscr{B}$ respectively. If $\mathscr{B}$ adheres to $\mathscr{R}$ through only the terminal cross section $\mathscr{D}_D$ we say $\mathscr{B}$ is *loosely bonded*—the curved contact surface is assumed to be lubricated or smooth. Finally, the bar supports a mass $m$ at $z = -(L-D)$ which at time $t$ is subjected to an oscillating force of low frequency $\omega$, $P_m e^{i\omega t}$, acting in the $z$-direction. We wish to determine then, for each bonding condition, the response of the bar to the applied loading.

We now consider the mass, bar and embedding medium for the fully-bonded case, beginning with the mass. If we interpret the system as a frequency-dependent spring-dashpot model the *equation of motion of the mass* can be expressed in the form

$$m\ddot{W} + c\dot{W} + kW = P_m e^{i\omega t}, \tag{1.1}$$

where $W(t)$ is the displacement of the mass, $c(\omega)$ the *equivalent damping coefficient*, $k(\omega)$ the *effective spring constant* and the dot denotes the operation $\mathrm{d}/\mathrm{d}t$. Since the forcing is harmonic and only the periodic solution is of concern here, $k + i\omega c$ is equal to the dynamic resistance of a given bar/embedding region configuration to a harmonic displacement of the mass with unit amplitude; in what follows we employ this interpretation and seek, in particular, $k$ and $c$.

In our analysis, attention is confined to long bars (viz. $d/L \ll 1$) excited at low frequencies thus allowing the use of an established first-order theory for longitudinal vibrations in a bar.

†A number of these investigations assume a viscoelastic embedding medium and thus add to the degree of damping. A nontrivial practical difficulty associated with such models is the determination of the viscoelastic parameters.

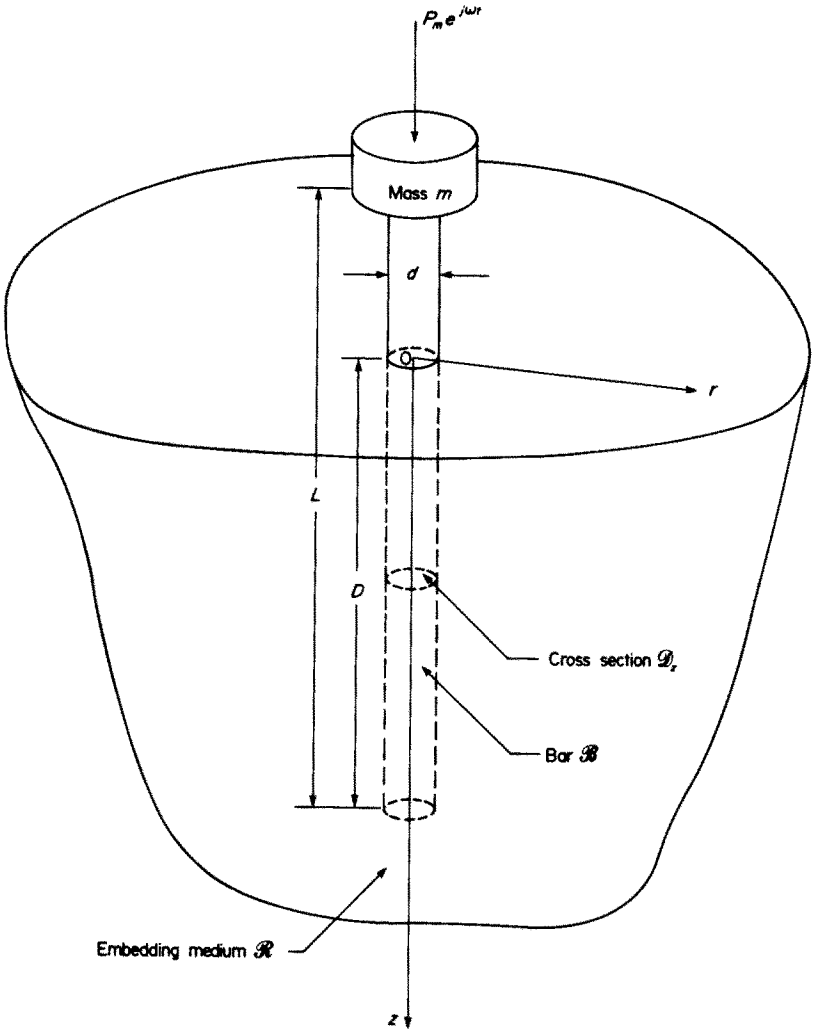


Fig. 1. Geometry of the mass, bar and embedding medium.

Hence the *governing equation for harmonic motion in the bar* is

$$\frac{d^2w}{dz^2} + k_b^2 w + \frac{4q}{\pi d^2 E} = 0, \tag{1.2}$$

for $-(L-D) < z < d$, where $w(z)\,e^{i\omega t}$ is the longitudinal displacement of the bar and $q(z)\,e^{i\omega t} = Q(z, t)$ is the shear force per unit length acting in the $z$-direction on the curved bar surface. Here $k_b = \omega/c_b$, $c_b = \sqrt{(E/\rho)}$ is the bar wave speed, $E$ Young's modulus of the bar and $\rho$ its mass-density. The *force-displacement relationship for the bar* is

$$p = \frac{\pi d^2 E}{4}\frac{dw}{dz}, \tag{1.3}$$

for $-(L-D) < z < D$, where $p(z)^{i\omega t} = P(z, t)$ is the axial bar force.

In treating the *boundary conditions for the fully-bonded case* it is convenient to analyze the projecting and embedded segments of the bar separately; accordingly let $\mathscr{B}_p$ denote the projecting segment of the bar, $\mathscr{B}_e$ the embedded segment and designate their respective cross sections at $z = 0$ by $\mathscr{D}_{O^-}$ and $\mathscr{D}_{O^+}$ (Fig. 2). The segment $\mathscr{B}_p$ has no shear stress on its curved boundary so that $q = 0$ in the governing equation of motion (1.2) for $-(L-D) < z < 0$. Since we wish to find the reaction at the bar head to a unit harmonic displacement of the mass, the

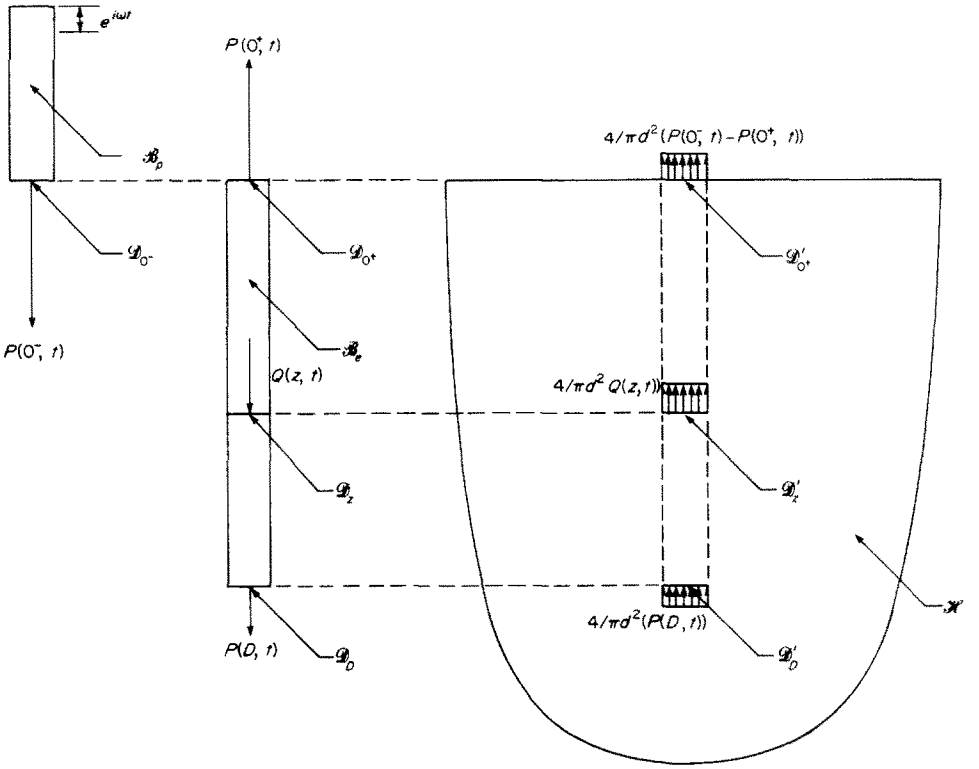


Fig. 2. Decomposition of the fully-bonded embedded-bar problem.

boundary condition there is†

$$w = 1 \text{ at } z = -(L - D). \tag{1.4}$$

The remaining boundary condition for $\mathscr{B}_p$ is found from *matching the force and displacement* across the cross sections $\mathscr{D}_{0^-}$ and $\mathscr{D}_{0^+}$ in the bar. This can be reduced to, on using (1.3),

$$w = \frac{4g_0}{\pi d^2} p(0^-) = Eg_0 \frac{\mathrm{d}w}{\mathrm{d}z} \text{ at } z = 0. \tag{1.5}$$

Here $p(0^-)\,\mathrm{e}^{i\omega t} = P(0^-, t)$ is the axial bar force applied to the disk $\mathscr{D}_{0^-}$ and $g_0(\omega)\,\mathrm{e}^{i\omega t}$ is the displacement of $\mathscr{B}_e$ at $z = 0$ when $p(0^-) = \pi d^2/4$, i.e. corresponding to a uniform axial stress oscillating with unit amplitude acting on $\mathscr{D}_{0^-}$. In order to find $g_0$ we now focus on the bar segments $\mathscr{B}_e$ and then the surrounding medium $\mathscr{R}$.

Recall that $\mathscr{B}_e$ is continuously bonded to the embedding medium throughout the interface $\partial\mathscr{R} \cap \partial\mathscr{B}$. As a result its cylindrical surface is subjected to a bond force per unit length $Q(z, t)$ $(0 < z < D)$ and the full equation of motion (1.2) holds. Also note that there is a possibility of direct load transfer to $\mathscr{R}$ at $z = 0$ with an associated discontinuity in the axial bar force between the cross sections $\mathscr{D}_{0^-}$ and $\mathscr{D}_{0^+}$ of magnitude say, $P(0^-, t) - P(0^+, t)$, where $P(0^+, t)$ is the portion of the axial bar force that is transmitted to $\mathscr{B}_e$. A further force acting on $\mathscr{B}_e$ is $P(D, t)$, the reaction induced by a displacement of the base (Fig. 2).‡ We now need to appraise the reactions to these forces in the embedding medium.

Unlike the pile, the region $\mathscr{R}$ must be treated as a three-dimensional continuum since our model relies on the spatial characteristics of the embedding medium for all the energy dissipation. However we can fill in the cavity in $\mathscr{R}$ with material of the same elastic properties

†Recall our earlier interpretation of $k$ and $c$.

‡In Fig. 2, the force directions indicated are the positive directions of the time-independent components of the forces, e.g. the direction of $P(0^-, T)$ is that of $p(0^-)$, $p(0^-) > 0$.

and yet still retain the essential three-dimensional nature.† In order to render the analysis tractable we make this approximation: we denote the full elastic half-space so formed by $\mathscr{H} = \{(r, z) | r \geq 0, z > 0\}$ and adopt the notations $\mathscr{D}_z'$ and $\mathscr{B}_e'$ for the regions in $\mathscr{H}$ which corresponds to $\mathscr{D}_z (0 < z \leq D)$ and $\mathscr{B}_e$ in $\mathscr{B}$. We simulate the effect of the bonding shear forces in $\mathscr{H}$ by uniformly distributed loads over $\mathscr{D}_z'$ whose magnitude per unit length of the $z$-axis is $-Q(z, t)$ $(0 < z < D)$. In addition, the reaction to any concentrated load transfer, $-(P(0^-, t))$, and the reaction to the end force, $-P(D, t)$, are represented by like load distributions over the respective cross sections $\mathscr{D}_O'$ and $\mathscr{D}_D'$.

What remains now is to ensure the perfect bonding between $\mathscr{B}_e$ and $\mathscr{H}$ throughout $\partial\mathscr{R} \cap \partial\mathscr{B}$. To this end we insist that the unknown forces $P(0^+, t)$, $P(D, t)$ and the force distribution $Q(z, t)$ induce the same displacement over $\mathscr{D}_z$ in $\mathscr{B}_e$ as the *average displacement* over $\mathscr{D}_z'$ in $\mathscr{B}_e'$. Consequently, if $\hat{w}(z, \zeta)\, e^{i\omega t}$ is the average displacement over the region $\mathscr{D}_z'$ in half-space in response to a uniform normal stress in the $z$-direction on $\mathscr{D}_\zeta'$, which oscillates with unit amplitude, the time-independent component of the displacement in the bar is given by

$$w(z) = \frac{4}{\pi d^2}\left([p(0^-) - p(0^+)]\hat{w}(z, 0) + p(D)\hat{w}(z, D) + \int_0^D q(\zeta)\hat{w}(z, \zeta)\, d\zeta\right), \tag{1.6}$$

for $0 \leq z \leq D$. An integral representation for the *displacement influence* function $\hat{w}$ is derived in the Appendix. Differential equations (1.2) and (1.3), together with the integral equation (1.6), govern the distributions of $w(z)$, $q(z)$ and $p(z)$. In the special case of $p(0^-) = \pi d^2/4$ then the $\lim_{z \to 0^+} w(z) = g_O$.

To conclude Section 1 we specialize the foregoing to the instance of the *loosely-bonded bar* wherein force-displacement matching applies only on $\mathscr{D}_D$ and $\mathscr{D}_D'$. The curved boundaries of the bar are taken to be smooth so that no shear forces are generated on the sides of the bar and $q = 0$ in the governing equation of motion (1.2) for $-(L - D) < z < D$. The boundary condition at the top of the bar remains the same as (1.4) while force-displacement matching at $z = D$ yields an analogous condition to that of (1.5), viz.

$$w = Eg_D \frac{dw}{dz} \text{ at } z = D, \tag{1.7}$$

where $g_D = \hat{w}(D, D)$, the displacement influence function evaluated at $z = \zeta = D$.

## 2. REPRESENTATIONS FOR $k$ AND $c$: INTEGRAL EQUATION FOR $p$

Here we derive an expression for the effective spring constant $k$ and the equivalent damping coefficient $c$ for the fully-bonded bar. This expression contains $g_O$, the time-independent component of the displacement at $z = 0$ induced by a normal stress which oscillates harmonically with unit amplitude and is uniformly distributed over $\mathscr{D}_O$. A little algebra enables $g_O$ to be expressed as a function of $p$, the time-independent component of the axial bar force, and establishes an integral equation for $p$. A numerical solution method for the integral equation is then described. The section concludes with an analogous though simpler development for the loosely-bonded bar.

The solution for the displacement $w$ in the *projecting* portion of the bar $\mathscr{B}_p$, governed by the equation of motion (1.2) with $q = 0$ and subject to the conditions in (1.4) and (1.5), may readily be shown to be

$$w = \frac{Eg_O k_b \cos k_b z + \sin k_b z}{Eg_O k_b \cos k_b(L - D) - \sin k_b(L - D)}, \tag{2.1}$$

for $-(L - D) \leq z \leq 0$. Recalling that $-p$ at $z = -(L - D)$ is the time-independent component of the reaction to a harmonic displacement of unit amplitude at the head of the bar and hence equivalent

†Note that a finite elastic filler cannot dissipate any energy in itself.

to $k + i\omega c$, eqn (2.1) together with the force-displacement relationship (1.3) give

$$k + i\omega c = \frac{\pi d^2 k_b E(\cos k_b(L-D) + k_b E g_O \sin k_b(L-D))}{4(\sin k_b(L-D) - k_b E g_O \cos k_b(L-D))}. \tag{2.2}$$

Equation (2.2) contains $g_O$, at present unknown. As remarked previously, $g_O = \lim_{z\to 0^+} w(z)$ when $p(0^-) = \pi d^2/4$ so its determination requires a knowledge of $w$ in the *embedded* portion of the bar $\mathscr{B}_e$; further $w$ is interrelated to $p$ and $q$ by the differential eqns (1.2) and (1.3) and the integral equation (1.6) and all three quantities are also unknown at present. We next seek to express $g_O$ in terms of $p$ and to eliminate $w$, $q$ from the set (1.2), (1.3) and (1.6) so as to furnish a means of determining $p$.†

We begin by eliminating $q$; $q$ may be removed from (1.6) by using (1.2) and (1.3). The integral equation so obtained is simplified by an integration by parts and can then be written as

$$w(z) + k_b^2 E\int_0^D w(\zeta)\hat{w}(z,\zeta)\,d\zeta = \frac{4}{\pi d^2}\left[p(O^-)\hat{w}(z,0) + \int_0^D p(\zeta)\frac{\partial \hat{w}}{\partial \zeta}(z,\zeta)\,d\zeta\right], \tag{2.3}$$

for $0 \leq z \leq D$. Now integrating (1.3) gives

$$w(z) = w(D) - \frac{4}{\pi d^2 E}\int_z^D p(\zeta)\,d\zeta, \tag{2.4}$$

for $0 \leq z \leq D$,‡ which on subsitution into (2.3) yields

$$w(z) + k_b^2 E w(D)\int_0^D \hat{w}(z,\zeta)\,d\zeta = \frac{4}{\pi d^2}\left[p(0^-)\,\hat{w}(z,0) + \int_0^D \left(p(\zeta)\frac{\partial \hat{w}}{\partial \zeta}(z,\zeta) + k_b^2 \hat{w}(z,\zeta)\int_\zeta^D p(\zeta')\,d\zeta'\right)d\zeta\right], \tag{2.5}$$

for $0 \leq z \leq D$. We can now express $g_O$ in terms of $p$: setting $z = D$ in (2.5) provides $w(D)$ which can be re-entered (2.4) and the limit as $z \to 0^+$ taken with $p(0^-) = \pi d^2/4$. Thus

$$g_O = \frac{\Delta}{k_b^2 E}\left[\hat{w}(D,0) + \int_0^D \left(\bar{p}(\zeta)\left(\frac{\partial \hat{w}}{\partial \zeta}(D,\zeta) - \frac{k_b^2}{\Delta}\right) + k_b^2 \hat{w}(D,\zeta)\int_\zeta^D \bar{p}(\zeta')\,d\zeta'\right)d\zeta\right]. \tag{2.6}$$

In (2.6), $\Delta = [(1/k_b^2 E) + \int_0^D \hat{w}(D,\zeta)\,d\zeta]^{-1}$, $\bar{p}(z) = p(z)/p(0^-)$ hereafter simply termed the *bar force*. It remains to establish an integral equation for $\bar{p}$ alone. This can be accomplished by removing $w(D)$ from (2.5) as earlier, differentiating the result with respect to $z$ and noting that [see Appendix (A7), (A9)–(A11)]

$$\frac{d}{dz}\int_0^D p(\zeta)\frac{\partial \hat{w}}{\partial \zeta}(z,\zeta)\,d\zeta = \int_0^D p(\zeta)\frac{\partial \hat{\gamma}}{\partial \zeta}(z,\zeta)\,d\zeta - 2p(z)\gamma_1(0),$$

for $0 \leq z \leq D$, then using the force-displacement relation (1.3) and dividing by $p(0^-)$ to arrive at:

$$[1/E + 2\gamma_1(0)]\bar{p}(z) = \hat{\gamma}(z,0) + \int_0^D \left(\bar{p}(\zeta)\frac{\partial \hat{\gamma}}{\partial \zeta}(z,\zeta) + k_b^2 \hat{\gamma}(z,\zeta)\int_\zeta^D \bar{p}(\zeta')\,d\zeta'\right)d\zeta$$
$$-\Delta\int_0^D \hat{\gamma}(z,\zeta)\,d\zeta\left[\hat{w}(D,0) + \int_0^D \left(\bar{p}(\zeta)\frac{\partial \hat{w}}{\partial \zeta}(D,\zeta) + k_b^2 \hat{w}(D,\zeta)\int_\zeta^D \bar{p}(\zeta')\,d\zeta'\right)d\zeta\right], \tag{2.7}$$

†The selection of $p$ as the survivor for determination is governed by two factors: firstly, $p$ may be a smoother function than $q$, since $q$ is proportional to $dp/dz$, and thus may be more amenable to numerical evaluation; secondly, the elimination of $w$ is algebraically easier to achieve than the elimination of $p$.

‡Initially it was thought that the expression of $w(z)$ in terms of $w(D)$ instead of $w(0)$ might aid the numerics since $w(D) \ll w(0)$; subsequent reflection indicates that the choice is probably arbitrary.

for $0 \leq z \leq D$. Equation (2.7) is the requisite *integral equation for the bar force* $\bar{p}$ in the embedded portion of the bar $\mathscr{B}_e$.

The numerical solution of (2.7) for $\bar{p}$ in $\mathscr{B}_e$ is found by means of a simple *finite-element* technique. We subdivide $\mathscr{B}_e$ into $N$ equal elements, namely the intervals $(i-1)D/N < z < iD/N$ $(i = 1, 2, \ldots N)$, and approximate $\bar{p}$ by the $N$ constants $\bar{p}_i (i = 1, 2, \ldots N)$ on these elements. Substituting this piece-wise constant approximation for $\bar{p}$ into the integral equation (2.7) and then demanding that the result holds at the mid-points of each of the elements, that is at $z = (2i-1)D/2N$ $(i = 1, 2, \ldots N)$, generates a set of $N$ linear equations in the $N$ unknowns, $\bar{p}_i$ $(i = 1, 2, \ldots N)$. The coefficients in this set contain double and even triple integrals; the inner infinite integrals stem from the representations for the influence functions [in eqns (A7), (A9) and (A11) of the Appendix] while the outer integrals and double integrals arise from integration along the embedded portion of the bar in (2.7, now discretized). Through a permissible interchange in the order, the integrals along the elements, and hence along the bar, can be found analytically; the remaining infinite integrals are evaluated numerically using the approach discussed in the Appendix. Then, with the aid of a standard routine for solving complex linear equations, we find an approximation for the bar force $\bar{p}$ and thus, via (2.6), $g_O$.

To ascertain the extent to which $\bar{p}$ must be discretized (i.e. the value of $N$) for $g_O$ to converge numerically, we considered a number of trial configurations. In the frequency range of interest, $0.04 \leq \omega d/2c_s \leq 0.5$, with the aspect ratio $D/d \leq 40$, it was found that the maximum difference between the bar force distribution calculated with $N = 8$ and that for $N = 16$ was only 3% while differences in $g_O$ were less than 6%. Consequently it appeared reasonable to proceed with 8 elements for aspect ratios less than or equal to 40. However, for the same frequency range but with $40 < D/d \leq 80$, at least 16 elements were required to obtain comparable convergence. The values so computed exhibited no evidence of any singular behavior in $p$ or its derivatives. Since unbounded stresses are a possibility near the surface in the original three-dimensional problem (see Bogy[6]), one can conclude that probably any such singular character has been incorporated in our approximate formulation as a contribution to the direct load transfer at $\mathscr{D}_O$. The numerical results derived from these values for a wide range of configurations for the fully-bonded bar are described in the next section.

Finally in this section we treat the *loosely-bonded bar.* The solution of the governing equation of motion for $w$ throughout $\mathscr{B}$, (1.2) with $q = 0$, satisfying the end conditions (1.4) and (1.7), gives, via the force-displacement relationship (1.3), the reaction at the head of the bar which in turn yields, on using our earlier interpretation,

$$k + i\omega c = \frac{\pi d^2 E k_b [\cos k_b L + k_b E g_D \sin k_b L]}{4[\sin k_b L - k_b E g_D \cos k_b L]}. \tag{2.8}$$

Equation (2.8) is the analogue of (2.2) for the fully-bonded bar: here, though, $g_D$ does not require the solution of an associated integral equation but can be determined directly as $\hat{w}(D, D)$ from the expression for $\hat{w}(z, \zeta)$ contained in eqns (A7) and (A9) of the Appendix. The results thus found for the loosely-bonded bar are also described in the next section.

## 3. RESULTS AND DISCUSSION

In this section we present selected results which illustrate the dependence of the spring constant and the damping coefficient on the forcing frequency and the physical quantities involved for both the fully-bonded and the loosely-bonded bars. Detailed results are given in [7].

To aid our presentation we identify the following set of *dimensionless parameters* which is sufficient to characterize any dynamic response of our system: $\bar{k} = 2k/\pi dE$ effective spring constant; $\bar{c} = 4cc_s/\pi d^2 E$ equivalent damping coefficient; $\bar{\omega} = \omega d/2c_s$ forcing frequency; $\bar{\delta}_1 = L/d$ bar aspect ratio; $\bar{\delta}_2 = D/d$ embedment aspect ratio; $\bar{s} = c_b/c_s$ wave speed ratio; $\bar{\rho} = \rho/\rho'$ density ratio; and $\nu$ = Poisson's ratio of the embedding medium. In the above recall that $E$ is Young's modulus for the bar, $c_b$ is the bar wave speed, $\rho$ the mass-density of the bar, and $c_s$ is the shear wave speed in the half-space; further note that $\rho'$ is the mass-density of the half-space.

In Fig. 3 then we consider the completely buried bar ($\bar{\delta}_1 = \bar{\delta}_2$) and show the variation of the spring constant $\bar{k}$ and damping coefficient $\bar{c}$ with *forcing frequency* $\bar{\omega}$ and *embedment aspect*

*ratio* $\bar{\delta}_2$. The values of the wave speed ratio ($\bar{s} = 30$) and the density ratio ($\bar{\rho} = 1.4$) are representative of a concrete/soil system, and Poisson's ratio of the embedding medium $\nu$ is taken to be 0.5 with some results for $\nu = 0.25$. In general, for the fully-bonded bar, both the stiffness and damping increase as $\bar{\delta}_2$ ranges from 5 to 80. We attribute this trend to the greater surface area (for a given diameter) available in the longer bars to resist motion and dissipate energy. This is in contrast to analyses entailing elastic strata overlying rigid half-space where $\bar{k}$ is inversely proportional to the aspect ratio $\bar{\delta}_2$ (see for example, Novak[8])—a consequence of an axially loaded bar with one end bonded to a rigid foundation since when the base of the bar is fixed the spring constant depends to a large extent on the axial stiffness of the bar itself rather than on the reaction induced in the embedding medium. Also we observe that the change in $\bar{c}$ and, to a lesser extent, that in $\bar{k}$, diminishes for aspect ratios $\bar{\delta}_2 > 20$; this tendency is more pronounced in "softer" bars (i.e. $\bar{s} < 30$). The stiffness and damping appear to be rather insensitive to Poisson's ratio in Fig. 3, a result indicating the dependence in general on $\nu$.

Variations in the spring constant and damping coefficient with $\bar{\omega}$ and *wave speed ratio* $\bar{s}$ are displayed for a typical bar/embedding medium ($\bar{\delta}_1 = 25$, $\bar{\delta}_2 = 20$, $\bar{\rho} = 1.4$, $\nu = 0.5$) in Fig. 4. For the fully-bonded case both $\bar{k}$ and $\bar{c}$ are quite sensitive to $\bar{s}$. Moreover, the dependence is even more appreciable for the loosely-bonded bar as this particular system has a resonant frequency at $\bar{\omega} = 0.44$ when $\bar{s} = 10$. This frequency provides abnormally large values of $\bar{c}$ and is the turning point of a sharp oscillation in $\bar{k}$. We remark that, for loosely-bonded bars with $\bar{\delta}_1 > 10$ and $10 < \bar{s} < 60$, resonance peaks similar to those of Fig. 4 may occur in the frequency range

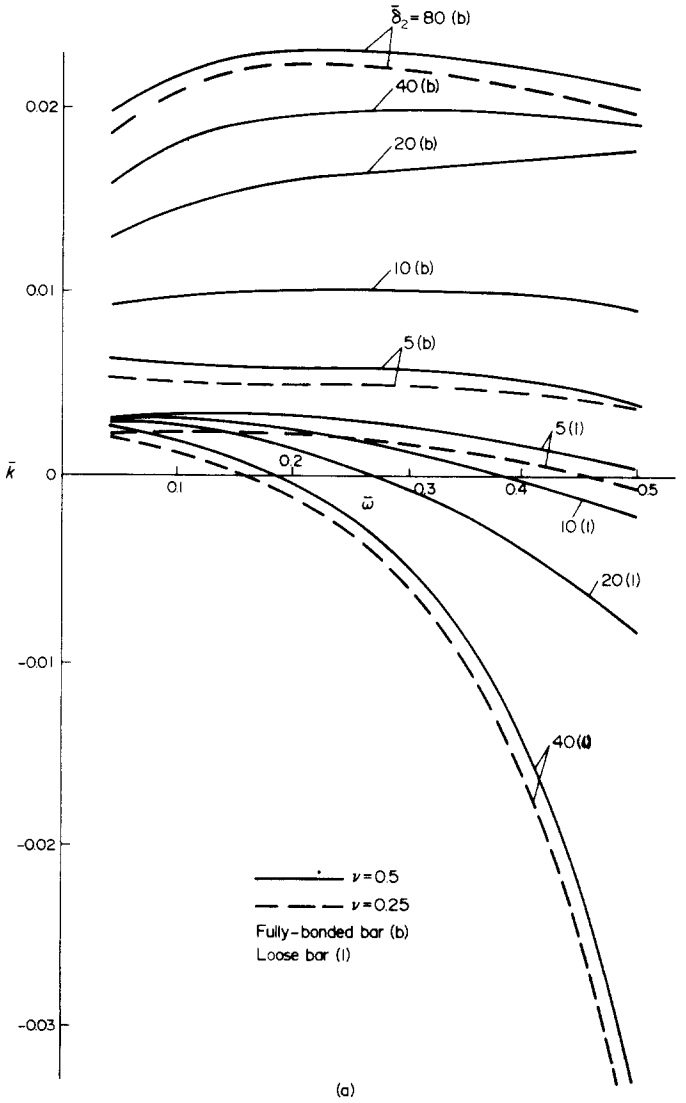

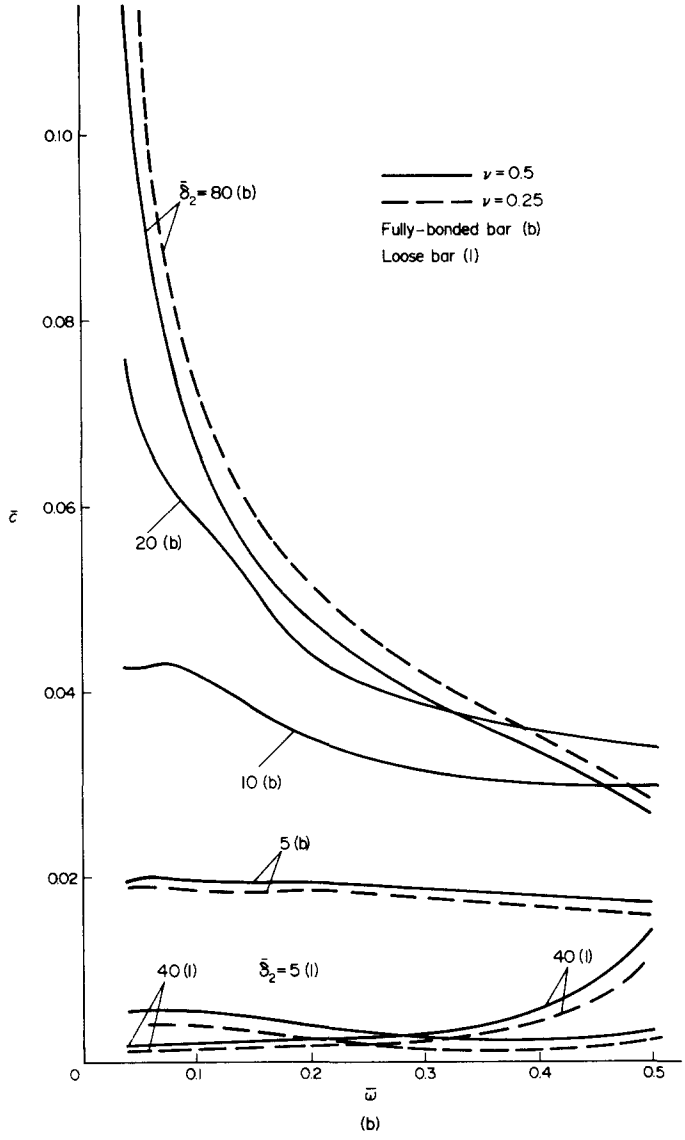


Fig. 3. Variation with frequency $\bar{\omega}$, aspect ratio $\bar{\delta}_2$ and Poissons ratio $\nu(\bar{\delta}_1 = \bar{\delta}_2, \bar{s} = 30, \bar{\rho} = 1.4)$: (a) stiffness $\bar{k}$; (b) damping $\bar{c}$.

considered here. However, like resonance phenomena are improbable for the fully-bonded bar in this frequency range unless $(\bar{\delta}_1 - \bar{\delta}_2) > 10$.

In Fig. 5 a bar/embedding medium configuration ($\bar{\delta}_1 = 25$, $\bar{\delta}_2 = 20$, $\bar{s} = 30$, $\nu = 0.5$) is depicted for varying *density ratios* $\bar{\rho}$. The range $0.2 < \bar{\rho} < 0.5$ reflects wood/soil systems while the range $0.9 < \bar{\rho} < 1.7$ corresponds to concrete/soil systems. The stiffness $\bar{k}$ is sensitive to changes in $\bar{\rho}$ while the damping $\bar{c}$ is relatively insensitive.

Finally, it is apparent from Figs. 3–5 that the spring constants and damping coefficients for the bar bonded at its base alone are significantly lower than those obtained for the fully-bonded case except near a resonant frequency. Accordingly the curves obtained may be used to provide an upper and lower bound on the energy dissipation. Further, bonding on the cylindrical pile surface tends to increase the resonant frequency and hence that found for the loosely-bonded bar can be regarded as the lower limit at which resonance may occur.

A related analysis awaiting future work is the flexural counterpart of our approach. The fundamental solutions required for this problem are for the displacements in the half-space in response to an oscillating distributed load applied tangentially to the disk $\mathcal{D}_\zeta$ and in response to an oscillating distributed moment on $\mathcal{D}_\zeta$—full three-dimensional elasticity problems of some complexity. These solutions would allow horizontal forces, bending moments and displace-

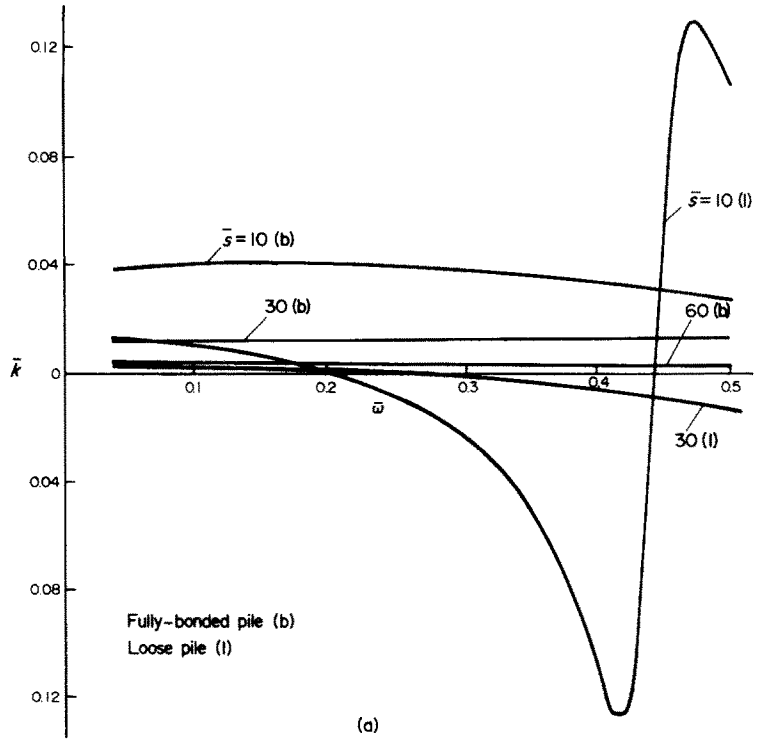


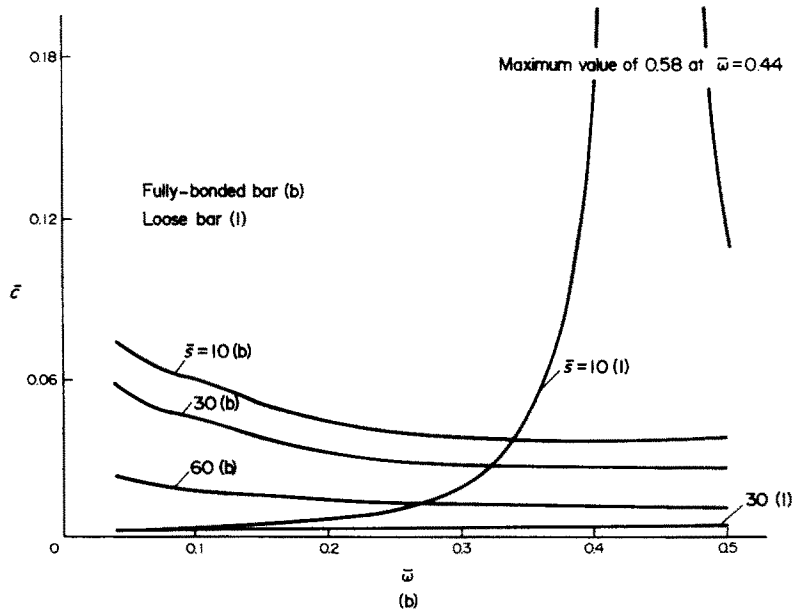


Fig. 4. Variation with frequency $\bar{\omega}$ and wave speed ratio $\bar{s}$ ($\bar{\delta}_1 = 25$, $\bar{\delta}_2 = 20$, $\bar{\rho} = 1.4$, $\nu = 0.5$): (a) stiffness $\bar{k}$; (b) damping $\bar{c}$.

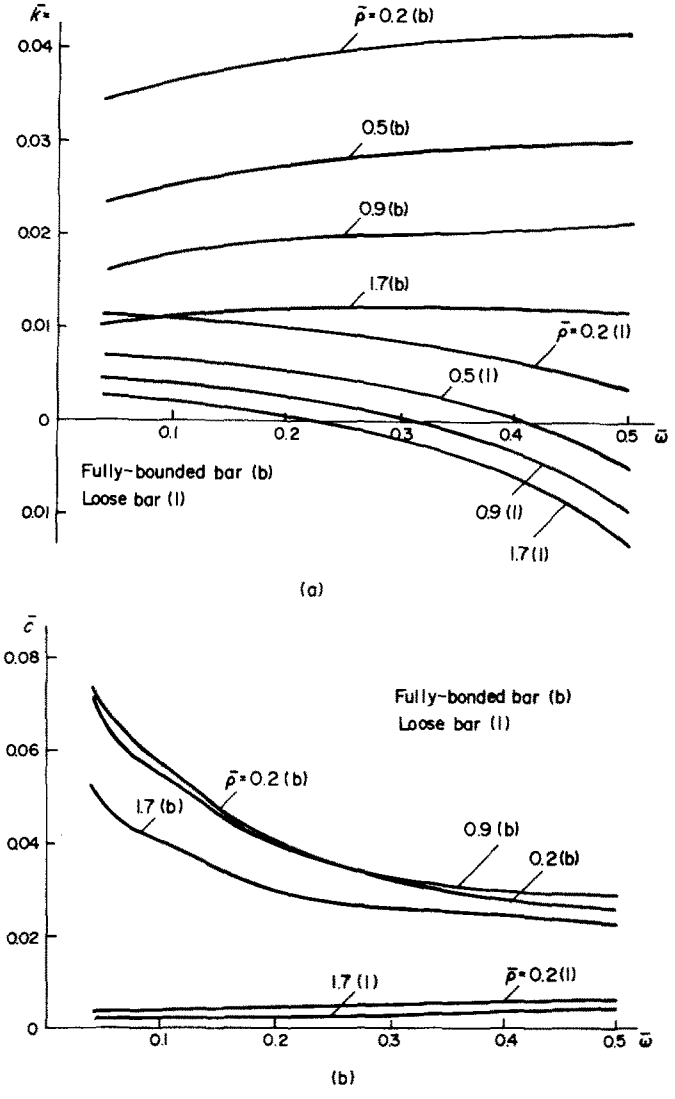


Fig. 5. Variation with frequency $\bar{\omega}$ and density ratio $\bar{\rho}(\bar{\delta}_1 = 25, \bar{\delta}_2 = 20, \bar{s} = 30, \nu = 0.5)$: (a) stiffness $\bar{k}$; (b) damping $\bar{c}$.

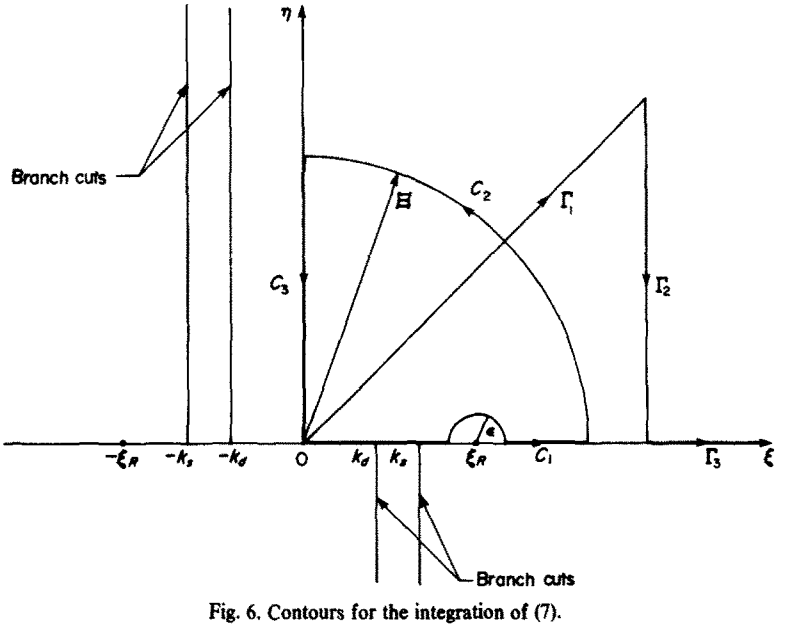


Fig. 6. Contours for the integration of (7).

ments to be matched between the bar and an approximate embedding medium in an analogous manner to the fully-bonded case presented here. Such an analysis would yield an equivalent lateral spring constant and damping coefficient for an embedded bar, information of considerable importance in the field of earthquake engineering.

*Acknowledgement*—The results communicated in this paper were obtained in the course of an investigation supported by the Structures Committee of the New Zealand National Roads Board.

## REFERENCES

1. A. H. Hadjian, J. E. Luco and N. C. Tsai, Soil-structure interaction: continuum or finite element? *Nuclear Engng Design* **31**, 151 (1974).
2. T. Nogami and M. Novak, Soil-pile interaction in vertical vibration. *Int. J. Earthquake Engng and Struct. Dyn.* **4**, 277 (1976).
3. E. Reissner, Stationäre, axialsymmetrische, durch eine schüttelnde Masse erregte Schwingungen eines homogenen elastischen Halbraumes. *Ingenieur-Archiv* **7**, 381 (1936).
4. G. Bycroft, Forced vibrations of a rigid circular plate on a semi-infinite elastic space and on an elastic stratum. *Phil. Trans R. Soc. Lond.* **A248**, 327 (1956).
5. R. Muki and E. Sternberg, Elastostatic load-transfer to a half-space from a partially embedded axially loaded rod. *Int. J. Solids Structures* **6**, 69 (1970).
6. D. B. Bogy, Two-bonded elastic wedges of different materials and wedge angles under surface tractions. *J. Appl. Mech.* **38**, 377 (1971).
7. G. F. Fowler and G. B. Sinclair, Dynamic Response of Embedded Piles under Vertical Loading. School of Engineering Report No. 152-TAM77/2, University of Auckland (1977).
8. M. Novak, Dynamic stiffness and damping of piles. *Can. Geotech. J.* **11**, 574 (1974).
9. C. L. Pekeris, The seismic surface pulse. *Proc. Nat. Acad. Sciences* **41**, 469 (1955).
10. H. Lamb, On the propagation of tremors over the surface of an elastic solid. *Phil. Trans R. Soc. Lond.* **A203**, 1 (1904).
11. M. Abramowitz and I. A. Stegun (Eds), *Handbook of Mathematical Functions*. Dover, New York (1965).

## APPENDIX

*Derivation of the half-space solutions*

Here we derive the displacement influence function $\hat{w}(z, \zeta)$ and the strain influence function $\hat{\gamma}(z, \zeta)$. The underlying half-space problem for the derivation entails the determination of the dynamic response of the half-space $\mathscr{H}$ to an oscillating body-force field, in the $z$-direction, which is uniformly distributed across a disk $\mathscr{D}'_\zeta$ within $\mathscr{H}$. We commence with a formulation of this problem in terms of Lamé potentials. We then introduce Hankel transforms to arrive at integral representations for $\hat{w}$ and $\hat{\gamma}$ and close with a description of the numerical evaluation of these representations.†

In what follows we suppress the $e^{i\omega t}$ multiplying factor throughout and refer to the time-independent quantities so generated simply by their original names, e.g. we agree to term $u_r$ the displacement in the radial direction when, in actuality, the displacement in the radial direction is $u_r e^{i\omega t}$. Thus satisfaction of the *axisymmetric displacement equations of harmonic motion* in the half-space is achieved on expressing $u_r(r, z)$, $u_z(r, z)$, the displacements in the $r$-, $z$-directions, through

$$u_r = \frac{\partial \phi}{\partial r} + \frac{\partial^2 \psi}{\partial r \partial z}, \quad u_z = \frac{\partial \phi}{\partial z} - \frac{1}{r}\frac{\partial}{\partial r}\left(r\frac{\partial \psi}{\partial r}\right), \tag{1}$$

on $\mathscr{H}$, where $\phi(r, z)$, $\psi(r, z)$ are the axisymmetric *Lamé potentials* governed by

$$\nabla^2 \phi + k_d^2 \phi = 0, \quad \nabla^2 \psi + k_s^2 \psi = 0, \tag{2}$$

on $\mathscr{H}$. In (2), $k_d = \omega/c_d$, $k_s = \omega/c_s$, $c_d$ is the dilational wave speed in $\mathscr{H}$, $c_s$ the shear wave speed and $\nabla^2$ is the axisymmetric laplacian operation. The *stress potential relations* required for our problem are:

$$\sigma_z = \lambda \nabla^2 \phi + 2\mu\left[\frac{\partial^2 \phi}{\partial z^2} - \frac{\partial}{\partial z}\left(\frac{1}{r}\frac{\partial}{\partial r}\left(r\frac{\partial \psi}{\partial r}\right)\right)\right],$$

$$\tau_{rz} = \mu\left[2\frac{\partial^2 \phi}{\partial r \partial z} + \frac{\partial^3 \psi}{\partial r \partial z^2} - \frac{\partial}{\partial r}\left(\frac{1}{r}\frac{\partial}{\partial r}\left(r\frac{\partial \psi}{\partial r}\right)\right)\right], \tag{3}$$

on $\mathscr{H}$, where $\sigma_z(r, z)$ and $\tau_{rz}(r, z)$ are normal and shear stress components, $\lambda$ and $\mu$ are Lamé constants for $\mathscr{H}$. The surface of the half-space is stress-free so that

$$\sigma_z = \tau_{rz} = 0 \text{ on } z = 0 \ (r \geq 0). \tag{4}$$

This *boundary condition* may be couched in terms of $\phi$, $\psi$ through (3). We incorporate the effect of the *body-force field* by viewing the half-space as composed of upper and lower regions divided by the plane $z = \zeta$ and inserting a discontinuity in

†Our approach has been employed previously in related problems on a number of occasions: in detail it most closely resembles the work of Pekeris who solves the problem of the half-space with a suddenly-applied, buried, point load *en route* to the problem of the surface point load in [9].

the normal stress $\sigma_z$ across a disk of diameter $d$ within this plane; that is we set

$$\sigma_z(r, \zeta^+) - \sigma_z(r, \zeta^-) = \begin{cases} 1 \text{ for } r < d/2 \\ 0 \text{ for } r > d/2, \end{cases} \tag{5}$$

with $u_r$, $u_z$, $\tau_{rz}$ continuous across $z = \zeta$. Via (3) again, (5) can be expressed in terms of $\phi$, $\psi$. To complete our formulation we take *conditions at infinity* which insist that the solution contain only outgoing waves as $Z \to \infty$, $Z = \sqrt{(r^2 + z^2)}$, and that the displacements vanish there. We seek then, $\phi$ and $\psi$ such that the preceding requirements are met, whence $u_z$ from (1), which in turn provides $\hat{w}$ *and* $\hat{\gamma}$.

To solve the wave equations (2) we use a *Hankel transform* on $r$ which naturally accommodates the axisymmetric laplacian operator and boundedness in the radial direction. We define the $n$th-order Hankel transform pair for $\phi$ by

$$\tilde{\phi}^n(\xi, z) = \int_0^\infty \phi(r, z) r J_n(\xi r)\, dr, \quad \phi(r, z) = \int_0^\infty \tilde{\phi}^n(\xi, z) \xi J_n(\xi r)\, dr, \tag{6}$$

where $J_n$ is the Bessel function of the first kind of order $n$; a completely analogous transform pair holds for any other function of $r$. Applying zeroth-order Hankel transforms to eqn (2) reduces them to ordinary differential equations in $z$ which may readily be solved in each of the two subregions of $\mathscr{R}$ (separated by the plane $z = \zeta$). The infinity conditions remove two of the "constants" in the lower region solution leaving six awaiting evaluation. Taking zeroth-order transforms of $u_z$ in (1) and $\sigma_z$ in (3), together with first-order transforms of $u_r$ in (1) and $\tau_{rz}$ in (3), furnishes $\tilde{u}_r^1$, $\tilde{u}_z^0$, $\tilde{\sigma}_z^0$ and $\tilde{\tau}_{rz}^1$ in terms of $\tilde{\phi}^0$, $\tilde{\psi}^0$. Now invoking the transform of the boundary conditions (4) at $z = 0$, the transform of the jump condition (5) at $z = \zeta$, and matching $\tilde{u}_r^1$, $\tilde{u}_z^0$, $\tilde{\tau}_{rz}^1$ at $z = \zeta$, provides the requisite six equations for the determination of the outstanding constants. Substituting the forms thus found for the Lamé potentials into (1) then leads to

$$u_z(r, z, \zeta) = \frac{d}{4\mu} \int_0^\infty [F_1(\xi, |z - \zeta|) + F_2(\xi, z, \zeta)/R^-(\xi)] J_1(\xi d/2) J_0(\xi r)\, dr, \tag{7}$$

on $\mathscr{H}$, where

$$F_1(\xi, |z - \zeta|) = (\alpha\beta\, e^{-\alpha|z-\zeta|} - \xi^2 e^{-\beta|z-\zeta|})/k_s^2\beta,$$
$$F_2(\xi, z, \zeta) = [R^+(\xi)(\alpha\beta\, e^{-\alpha(z+\zeta)} + \xi^2 e^{-\beta(z+\zeta)}) - \kappa(e^{-(\alpha z+\beta\zeta)} + e^{-(\beta z+\alpha\zeta)})]/k_s^2\beta,$$
$$R^\pm(\xi) = (2\xi^2 - k_s^2)^2 \pm 4\xi^2\alpha\beta,$$

with

$$\kappa = 4\xi^2\alpha\beta(2\xi^2 - k_s^2), \quad \alpha = \sqrt{(\xi^2 - k_d^2)}, \quad \text{and} \quad \beta = \sqrt{(\xi^2 - k_s^2)}.$$

The properties of the integrand in (7) warrant investigation at this stage. First note that $R^- = 0$, the *Rayleigh wave equation*, has real roots at, say, $\xi = \xi_R$ for the physical range of Poisson's ratio; for example, for Poisson's ratio of 1/4, $\xi_R = \pm(3 + \sqrt{3})^{1/2} k_s/2$. Accordingly there is a simple pole on the path of integration in (7); we choose the path around the pole so as to produce only waves which propagate radially outwards, i.e. waves of the form $e^{\pm i(\xi r - \omega t)}$. With this in mind, a decomposition of the Bessel function $J_0(\xi r)$ into Hankel functions of the first and second kinds together with an inspection of the asymptotic behavior of these Hankel functions for large arguments, and an application of the Cauchy integral theorem to the contour $C = C_1 + C_2 + C_3$ in the complex plane of $\xi + i\eta$ (Fig. 6), leads to the selection of $C_1$ as $\epsilon \to 0$, $\Xi \to \infty$ as the appropriate integration path. Here $C_1$ prior to the dual limiting process consists of the two linear segments $(0, \xi_R - \epsilon)$, $(\xi_R + \epsilon, \Xi)$ and the semicircular path of radius $\epsilon$ in the positive $\eta$ half-plane which circles above $\xi = \xi_R$, and $\Xi = \sqrt{(\xi^2 + \eta^2)}$.†

Further investigation of the integrand in (7) reveals that, in addition to the simple pole at $\xi = \xi_R$, it has square-root singularities at $\xi = \pm k_s$ and branch-points at $\xi = \pm k_s, \pm k_d$. To avoid these last singularities on the path of integration we again make recourse to Cauchy's integral theorem and trade in $C_1$ (under $\epsilon \to 0$, $\Xi \to \infty$) for $\Gamma = \Gamma_1 + \Gamma_2 + \Gamma_3$ (Fig. 6). Thus $\int_\Gamma$ replaces $\int_0^\infty$ in (7) and we have a path of integration which is free from any singularities and ensures only outward propagating waves.

The *displacement influence function* $\hat{w}$ is defined as the average vertical displacement over the disk $\mathscr{D}_z'$ in our half-space problem, i.e.

$$\hat{w}(z, \zeta) = \frac{8}{d^2} \int_0^{d/2} u_z(r, z, \zeta) r\, dr, \tag{8}$$

for $0 \leq z \leq D$, $0 \leq D$. Hence from (7), on making the permissible change in the order of integration, we have

$$\hat{w}(z, \zeta) = \frac{1}{\mu} \int_\Gamma [F_1(\xi, |z - \zeta|) + F_2(\xi, z, \zeta)/R^-(\xi)] J_1^2(\xi d/2) \frac{d\xi}{\xi}, \tag{9}$$

for $0 \leq z \leq D$, $0 \leq \zeta \leq D$.‡ Thus (9) is the integral representation sought for $\hat{w}$ and the integral representation for the *strain influence function* $\hat{\gamma}$ follows from (9) and the definition of $\hat{\gamma}$ by

$$\hat{\gamma}(z, \zeta) = \frac{\partial \hat{w}}{\partial z}(z, \zeta), \tag{10}$$

for $0 \leq z \leq D$, $0 \leq \zeta \leq D$, and is given by

$$\hat{\gamma}(z, \zeta) = \operatorname{sgn}(z - \zeta) \hat{\gamma}_1(|z - \zeta|) + \hat{\gamma}_2(z, \zeta),$$

†A detailed explanation of this selection process is given in [7], the basic approach being developed by Lamb in [10].

‡In establishing (9), and later (13), we have used results that can be found in, for example [11, Chap. 11].

for $0 \leq z \leq D$, $0 \leq \zeta \leq D$, where

$$\hat{\gamma}_1(|z-\zeta|) = \mu \int_\Gamma F_3(\xi, |z-\zeta|) J_1^2(\xi d/2) \frac{d\xi}{\xi},$$

$$\hat{\gamma}_2(z, \zeta) = \mu \int_\Gamma [F_4(\xi, z, \zeta) J_1^2(\xi d/2)/\xi R^-(\xi)]\, d\xi,$$

$$F_3(\xi, |z-\zeta|) = (\xi^2 e^{-\beta|z-\zeta|} - \alpha^2 e^{-\alpha|z-\zeta|})/k_s^2,$$

$$F_4(\xi, z, \zeta) = -[R^+(\xi)(\alpha^2\beta e^{-\alpha(z+\zeta)} + \xi^2\beta e^{-\beta(z+\zeta)}) - \kappa(\alpha e^{-(\alpha z+\beta\zeta)} + \beta e^{-(\beta z+\alpha\zeta)})]/k_s^2\beta,$$

and sgn is the signum function.

Analytical evaluation of these integral representations cannot be readily achieved; however their numerical evaluation is straightforward. An iterative, complex, trapezoidal rule over approximately equal subintervals of $\Gamma$ suffices to evaluate both $\hat{w}$ and $\hat{\gamma}$. Integration along $\Gamma_3$ is terminated when contributions to the integral from successive subintervals contribute less than 0.5% of its cumulative value. Convergence is aided on $\Gamma_3$ on realizing that

$$F_1(\xi, |z-\zeta|) J_1^2(\xi d/2)/\xi \approx -(k_d^2 + k_s^2) J_1^2(\xi d/2)/(2k_s^2\xi^2) \text{ -a } \xi \to \infty, \tag{12}$$

and that

$$\int_0^\infty J_1^2(\xi d/2) \frac{d\xi}{\xi^2} = \frac{2d}{3\pi}. \tag{13}$$

Using these observations, the dominant component of the integrands for large $\xi$ can be subtracted off, thereby generating more rapidly decaying functions which can be integrated numerically then combined with the analytical contributions from (13). The use of this last technique enabled rapid numerical evaluations of the integral representations to be made.